Hindawi Publishing Corporation
Mathematical Problems in Engineering
Volume 2015, Article ID 242431, 9 pages
http://dx.doi.org/10.1155/2015/242431

Research Article

Fault Detection Based on Tracking Differentiator Applied on the Suspension System of Maglev Train

Hehong Zhang, Yunde Xie, and Zhiqiang Long

College of Mechatronics Engineering and Automation, National University of Defense Technology, Changsha, Hunan 410073, China

Correspondence should be addressed to Zhiqiang Long; zhqlong@263.net

Received 1 October 2014; Accepted 26 January 2015

Academic Editor: Francesco Braghin

A fault detection method based on the optimized tracking differentiator is introduced. It is applied on the acceleration sensor of the suspension system of maglev train. It detects the fault of the acceleration sensor by comparing the acceleration integral signal with the speed signal obtained by the optimized tracking differentiator. This paper optimizes the control variable when the states locate within or beyond the two-step reachable region to improve the performance of the approximate linear discrete tracking differentiator. Fault-tolerant control has been conducted by feedback based on the speed signal acquired from the optimized tracking differentiator when the acceleration sensor fails. The simulation and experiment results show the practical usefulness of the presented method.

1. Introduction

Maglev train is a new kind of urban railway system that has advantages of lower noise, less exhaust fumes emission, and less maintenance cost. It is under engineering application now in many countries, such as China, Japan, and Korea [1–3]. According to the engineering application, the acceleration sensor is the main cause for the suspension system fault due to its direct installation on the electromagnet and its poor external operating environment. The suspension control system cannot guarantee the suspension stability without the speed signal obtained by acceleration sensor. How to obtain the fault information of acceleration sensor timely and conduct fault-tolerant control promptly is important to guarantee the safety and stability of the maglev train [4–6]. With the rapid development and enormous advantages of maglev train, the research on the fault detection for the suspension control system is both theoretically and practically significant. This is also the starting point of this paper.

In accordance with the existing public documents, the research both at home and abroad on the fault detection of the suspension control system is very few. Instead, most of the studies focus on the system modeling, analysis, and the controller design. At home, the research on the fault detection mainly focuses on aspects of power supply, traction subsystem, and the safe reliability analysis of suspension system [7, 8]. Michail et al. [9] studied the fault detection of the gap sensor of suspension system and it was conducted by comparing the gap measurement value, the estimated value of Kalman filtering, the gap value computed on electric current, and magnetic flux density. Also, a research on the fault detection of the acceleration sensor, gap sensor, and the actuator of a monopodium double-iron suspension system has been conducted by some researchers from Korea, including Sung and Kim [10–12]. The research detects the fault by obtaining one residual through comparing the measurement value of the gap and the acceleration with the gap and acceleration value computed on the basis of the system input signal and electromagnet current value. Then the other residual through comparing the currents of two electromagnets is obtained. The fault indicator of this component through adding the mean values of the square of one residual with the square of the other residual according to certain algorithm can be worked out. Finally it can get the fault detection result by performing fuzzy theory algorithm on this indicator and its derivative. While the research at home [13] primarily focuses on the fault-tolerant plan for the sensor and actuator of the suspension system, the methods of Kalman filtering,

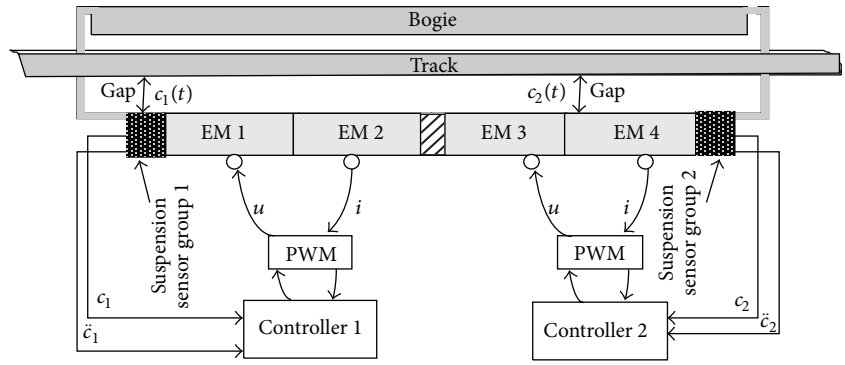

Figure 1: Suspension control system of the module.

strong tracking filtering, and full-dimension observer are applied after the suspension control system is linearized at the equilibrium point. And then the fault is detected by checking the parameters and states of system before and after the fault.

In view of the existing methods, this paper focuses on the fault detection for the acceleration sensor of the suspension system in the maglev train. If model-based fault detection method [14] is employed, the detection effect will be greatly discounted because the mathematical model of suspension system cannot be obtained accurately. If knowledge-based fault detection method [15] is taken, the suspension system would not be very applicable due to the lack of prior knowledge of fault. Consider that many faults will affect the measurement of signal (generally the input/output signal) and change some of their features in practical system. The method based on processing the input/output signal analyzes the features of the detectable signal, such as the correlation function, frequency spectrum, higher-order statistics, and autoregression moving average process. By observing the change of features of the signal or comparing the redundancy signal, it can infer the fault model and then realize fault detection. By optimizing the approximate linear tracking differentiator proposed by Han and Yuan [16] (hereinafter referred to as *Ftd*) and extracting the speed signal as the reference signal with *Ftd* algorithm, this paper compares the reference signal with the acceleration sensor signal. And then the fault of the acceleration sensor is detected by the threshold value that is set by introducing the Bayesian Decision Theory [17, 18] for comparison result. The fault-tolerant control is performed by introducing the speed signal acquired by the optimized linear tracking differentiator when fault occurs.

2. Analysis of the Structure and Problem of the Suspension Control System in Maglev Train

2.1. Structure of the Suspension. Maglev train is an integrated electromechanical system composed of vehicle structure, bogie, track, suspension controller, and suspension sensor group, and so forth. As shown in Figures 1-2, the four electromagnets (EM) of suspension control system are controlled by two controllers. The unit of PWM exerts ultimate voltage on the electromagnets. Each controller corresponds to two series connected electromagnets. Controller 1 and Controller 2, respectively, receive the signal of the sensor group on the left side and the right side. There are three redundancy gap sensors and one acceleration sensor in one sensor group.

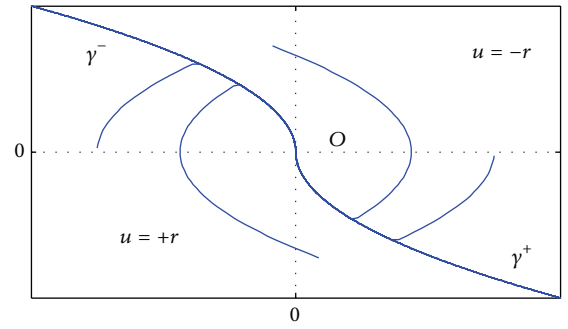

Figure 2: Illustration of the switching curve and the optimal trajectory.

2.2. Problem of the Suspension System. The closed loop feedback control is realized through gap signal, vertical velocity signal, and current signal in the suspension control system. These feedback signals are, respectively, provided by gap sensor, the integral of signal of acceleration sensor, and current sensor. In maglev train project, the fault probability of current sensor is lower because the sensor is installed inside the crate and possesses a good operating condition. To solve the problem of gap connection, the gap sensor uses triplication redundancy configuration so that fault in one gap sensor would not affect the acquisition of the gap signal. In order to acquire the vibration information in the suspension electromagnet, the acceleration sensor is installed on the electromagnet. As a result, it is more likely to fail [6]. Therefore, this paper mainly targets the fault detection of the acceleration sensor.

The core of fault detection by means of signal processing is to find a relatively stable velocity reference signal before and after the fault. Having a low fault probability due to its adoption of triplication redundancy configuration in maglev project, the reference signal can be required from gap sensor. And then fault detection of the acceleration sensor can be conducted by comparing the reference signal and the integral

of the acceleration sensor signal. In this paper, the velocity signal of system is acquired by using the tracking differentiator. Tracking differentiator with obvious flutter phenomenon and requirement of high-frequency adjustment of control variable is unacceptable for the practical control system because the high-frequency change needs to consume much energy and the high-frequency perturbation of tracking signal indicates the abrasion of mechanical device. Therefore, this paper aims at optimizing the parts that have overshoot, error, or flutter phenomenon on the basis of the approximate linear tracking differentiator proposed by Han and Yuan [16]. By optimizing the deviation of control algorithm wherever the states locate within or beyond the two-step reachable region, the flutter problem can be solved. And an approximate linear tracking differentiator (hereinafter referred to as *Ftd*) that does not contain the square roots algorithm and whose form is simple and whose implement action is easy can be acquired.

3. An Optimized Approximate Linear Tracking Differentiator Algorithm

According to part 2, the key to the fault detection of the acceleration sensor for the suspension system of maglev train is to obtain the efficient velocity signal as the reference signal. Gaining the differential signal rapidly and accurately and restraining the noise in the signal have always been an important topic. Tracking differentiator (TD) can track the input signal and extract of appropriate differential signal effectively, which make it increasingly popular among researchers. Khalil and some other researchers [19, 20] designed a linear high-gain differentiator, which provides the derivatives of signal from 1 to $(n-1)$. The tracking differentiator based on bang-bang control is actually a kind of sliding differentiator. Researchers such as Levant [21–24] and Utkin [25, 26] have done a series of studies on the features of sliding differentiator. They applied this differentiator to filtering, sliding-mode control, parameter estimation, and so forth and have obtained certain achievements. Han and Yuan [16] proposed a discrete tracking differentiator based on the second order time-optimal control system and applied it to active-disturbance-rejection control (ADRC) [27]. It solves the complex problems of disturbance observation, tracking control, and parameter estimation better and has a good robust stability. In the meantime, Xie proposed a second-order nonlinear discrete tracking differentiator based on the research of Han that is able to amend its characteristic points and is flexible to applications. And Xie applied this differentiator to the velocity and position detection of a permanent magnet electrodynamic maglev train system [28]. To simplify the discrete tracking differentiator, Han [29] proposes a kind of approximate linear discrete tracking differentiator in his book *Active-Disturbance-Rejection Controller: Compensation Technology*, taking the features of two-step reachable region and the reversion of switching curve into consideration. However, the tracking trajectory obtained according to the final formula in this book has problems of overshoot and flutter, which makes it difficult to promote and apply. This part discusses the simplification of the approximate linear and points out the disadvantage of the approximate linear formula in [29]. Finally this part gives an optimized approximate linear discrete formula. The simulation results show error between the TD of Han and the two other different linear approximate formulas, respectively.

3.1. Synthesis Function of Second-Order Discrete Time-Optimal Control System. In accordance with the optimal control theory, the time-optimal control of the second-order integrator system with the starting point as the terminal one is bang-bang control [30]. And the model of the second-order system can be written as

$$\begin{aligned} \dot{x}_1 &= x_2, \\ \dot{x}_2 &= u, \quad |u| \le r. \end{aligned} \tag{1}$$

The switching curve of the bang-bang control can be given by

$$\Gamma(x_1, x_2) = x_1 + \frac{x_2 |x_2|}{2r}. \tag{2}$$

Control strategy that is shown in Figure 2 can be defined as

$$u = -r \operatorname{sgn}(\Gamma(x_1, x_2)). \tag{3}$$

When the second-order integrator system is dispersed simply, the system would generate unsatisfactory high-frequency flutter after it stabilizes. It is a challenge to both the study and application of rapid tracking differentiator. A further research on the reasons for flutter is a must. The boundary characteristic curves of linear regions with the second-order discrete time-optimal control are presented using the method of the state back step by Han. And by means of it, Han designed a brilliant method that avoided the flutter. According to the algorithm of the discrete tracking differentiator in document [29], it can be assumed that the discrete step is h, any point on the phase plane is $M(x_1, x_2)$, and then the discretionary result of (1) is (4). And the control force u is determined by (5). The algorithm (herein referred to as *Fhan*) formula can be written as

$$\begin{aligned} &x_1(k) = x_1(k) + hx_2(k), \\ &x_2(k) = x_2(k) + hu(k), \\ &|u(k)| \le r, \ k = 0, 1, 2, \ldots \end{aligned} \tag{4}$$

$$\begin{aligned} &\Omega_r = \left\{ |x_1 + hx_2| \le h^2 r \cap |x_1 + 2hx_2| \le h^2 r \right\} \\ &\text{if} \cdot M \subseteq \Omega_r \\ &u = -\frac{x_1 + 2hx_2}{h^2} \\ &\text{else} \\ &y = x_1 + hx_2 \\ &g(x_1, x_2) = x_2 - \left(\frac{hr}{2} - \frac{1}{2} \sqrt{h^2 r^2 + 8r|y|} \right) \operatorname{sgn}(y) \\ &u = -r \cdot \operatorname{sat}(g(x_1, x_2), hr) \\ &\text{end.} \end{aligned} \tag{5}$$

Removing the "if" statement in formula (5), the formula can be adapted as follows by using the sign function:

$$
\begin{aligned}
&d = rh^2, \qquad a_0 = hx_2, \qquad y = x_1 + a_0,\\
&a_1 = \sqrt{d\left(d + 8\left|y\right|\right)},\\
&a_2 = a_0 + \frac{\operatorname{sign}\left(y\right)\left(a_1 - d\right)}{2},\\
&S_y = \frac{\left(\operatorname{sign}\left(y + d\right) - \operatorname{sign}\left(y - d\right)\right)}{2},\\
&a = \left(a_0 + y - a_2\right) S_y + a_2,\\
&S_a = \frac{\left(\operatorname{sign}\left(a + d\right) - \operatorname{sign}\left(a - d\right)\right)}{2},\\
&Fhan = -r\left(\frac{a}{d} - \operatorname{sign}\left(a\right)\right) S_a - r\operatorname{sign}\left(a\right).
\end{aligned}
\tag{6}
$$

Apparently, formula (6) contains the square roots algorithm, which complicated the whole algorithm and increased the calculation. This is inefficient for the practical engineering application. In formula (5), Ω_r is the two-step reachable region, which is a rhombus circled by four points: $(-h^2r, 0)$, $(-3h^2r, 2hr)$, $(h^2r, 0)$, and $(3h^2r, -2hr)$, as shown in Figure 3, the region circled by blue line. $g(x_1, x_2)$ is the boundary transfer function and $\mathrm{sat}(x, \delta)$ is the standard saturation function. The sketch map of the switching curve, two-step reachable region, and the optimal trajectory is shown in Figure 3.

3.2. Boundary Simplification and Approximate Linear Representation. Without considering the boundary layer thickness, it can simplify the boundary and get the switching curve under discretization as follows:

$$
\Gamma_0\left(x_1, x_2\right) : x_1 + \frac{x_2\left|x_2\right|}{2r} + \frac{1}{2}hx_2 = 0. \tag{7}
$$

In accordance with the method in document [16] the quasi-linear algorithm is expressed as follows:

$$
\begin{aligned}
&d = h^2r, \qquad z_1 = x_1 + hx_2,\\
&z_2 = z_1 + hx_2, \qquad a = x_1 + \frac{x_2\left|x_2\right|}{2r} + \frac{1}{2}hx_2,\\
&S_1 = \frac{\left(\operatorname{sgn}\left(z_1 + d\right) - \operatorname{sgn}\left(z_1 - d\right)\right)}{2},\\
&S_2 = \frac{\left(\operatorname{sgn}\left(z_2 + d\right) - \operatorname{sgn}\left(z_2 - d\right)\right)}{2},\\
&S_c = S_1S_2, \qquad U_Z = -\frac{z_2}{h^2}, \qquad U_a = -r\operatorname{sgn}\left(a\right),\\
&u = S_cU_z + \left(1 - S_c\right)U_a.
\end{aligned}
\tag{8}
$$

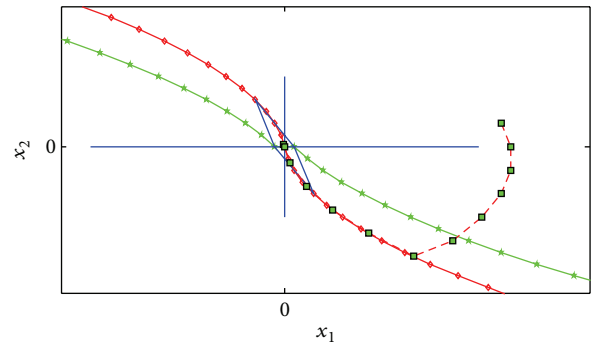

Figure 3: Illustration of the reachable area, switching curve, and the optimal trajectory.

And according to the book of Han [29], the approximate TD is expressed as follows:

$$
\begin{aligned}
&d = h^2r, \qquad a_0 = hx_2,\\
&y = x_1 + a_0, \qquad z = y + a_0,\\
&a = y + \frac{a_0\left(\left|a_0\right|/d - 1\right)}{2},\\
&S_y = \frac{\left(\operatorname{sgn}\left(y - d\right) - \operatorname{sgn}\left(y + d\right)\right)}{2},\\
&S_z = \frac{\left(\operatorname{sgn}\left(z - d\right) - \operatorname{sgn}\left(z + d\right)\right)}{2},\\
&u = -r\left(z - \operatorname{sign}\left(z\right) - \operatorname{sign}\left(a\right) S_yS_z + \operatorname{sign}\left(z\right) + \operatorname{sign}\left(a\right)\right).
\end{aligned}
\tag{9}
$$

To further discuss formula (9), a conclusion can be drawn that if $M(x_1, x_2)$ on the phase plan is within the two-step reachable region, namely, $|y| \le d \cap |z| \le d$, $M \subseteq \Omega_r$, then it can obtain that $S_yS_z = 1$, $u = -r_z$. But the actual algorithm should be $u = -z/h^2$ by computation when $M(x_1, x_2)$ is within the two-step reachable region. Besides, taking the point beyond the two-step reachable region into account, namely, $S_yS_Z = 1$, $u = -r(\mathrm{sgn}(z) + \mathrm{sgn}(a))$, the actual reversion algorithm is $u = -r\,\mathrm{sgn}(a)$, so naturally difference also exists here. Therefore, the conclusion can be drawn that the approximate linear algorithm (9) in document [29] is partially erred and the right algorithm should be formula (8).

According to the analysis of formula (9), there is a redundant $\mathrm{sgn}(z)$ both within and beyond the reachable region and factor d is missing for the item with z. The correct formula is as follows:

$$
u = -r\left(\frac{z}{d} - \operatorname{sgn}\left(a\right) S_yS_z + \operatorname{sgn}\left(a\right)\right). \tag{10}
$$

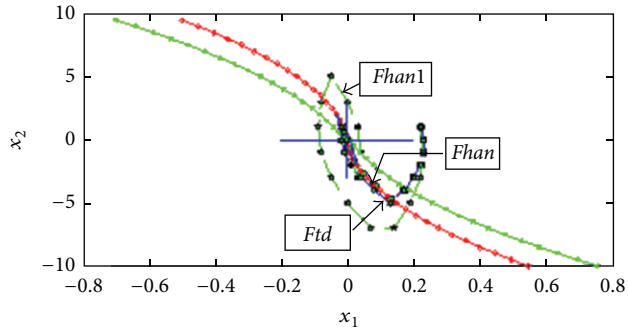

FIGURE 4: Illustration of trajectory of three different TD algorithms.

The result now is the same as that of (8) and formula (9) can be revised as

$$d = h^2 r, \qquad a_0 = h x_2,$$
$$y = x_1 + a_0, \qquad z = y + a_0,$$
$$a = y + \frac{a_0 \left(|a_0| / d - 1\right)}{2},$$
$$S_y = \frac{\left(\operatorname{sgn}\left(y + d\right) - \operatorname{sgn}\left(y - d\right)\right)}{2}, \tag{11}$$
$$S_z = \frac{\left(\operatorname{sgn}\left(z + d\right) - \operatorname{sgn}\left(z - d\right)\right)}{2},$$
$$u = -r\left(\frac{z}{d} - \operatorname{sgn}\left(a\right) S_y S_z + \operatorname{sgn}\left(a\right)\right).$$

Formula (11) is completely equal to formula (8), which is a correction of formula (9). Thus, this formula shows the disadvantage of document [29] by Han and corrects the shortcoming.

3.3. Comparison of the Numerical Simulation Result. To compare the errors of the two approximates against the TD of Han, we can compare the phase path of a point on the phase plane firstly and then study the difference with the tracking input signal and differential signal.

(1) The Time-Optimal Trajectory on the Phase Plane.

TD algorithm of Han is formula (6) and here is expressed as *Fhan*. Its approximate algorithm before correction is formula (9) which is recorded as *Fhan*1. And the new approximate algorithm (11) is displayed as *Ftd*. The result is as shown in Figure 4.

As shown in Figure 4, algorithm *Fhan*1 (formula (9)) deviated from the switching curve with overshoot and winding phenomenon, which is largely different from *Fhan*. But algorithm *Ftd* is slightly deviated from the switching curve and has slight deviation with algorithm *Fhan*. According to Figure 3, the algorithm of *Ftd* that is the approximate one of TD is a feasible linear approximate algorithm. But formula (10) is largely deviated, which is apparently disadvantaged.

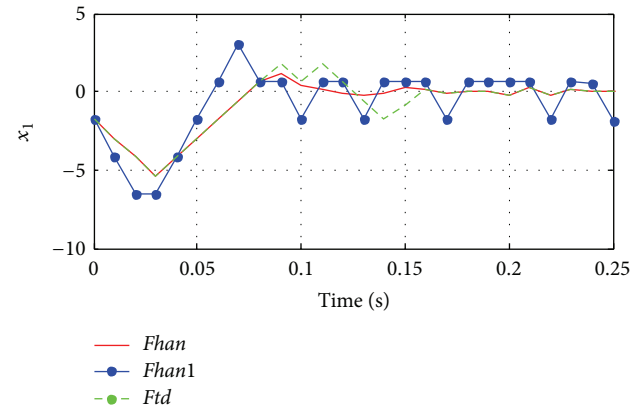

FIGURE 5: Illustration of the comparison of the tracking error of input signal.

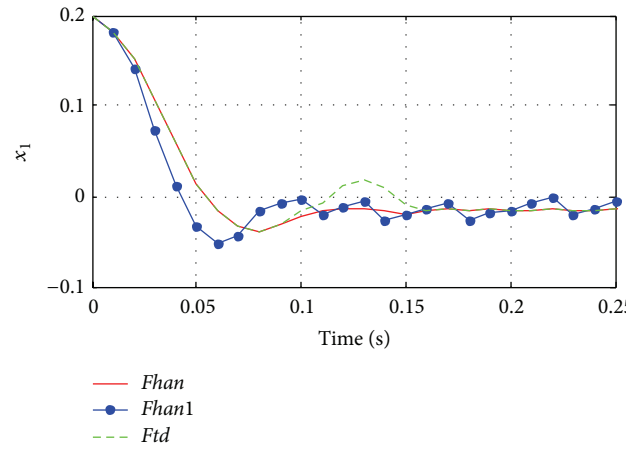

FIGURE 6: Illustration of the comparison differential error of the input signal.

(2) The following simulation is the comparison for three different TD algorithms (*Fhan*1 *Fhan Ftd*) by using a common input signal to illustrate the ability of tracking input signal and extracting relevant differential signal of them.

It is defined as follows: input signal as $v(t) = \sin(0.25\pi t) + \gamma(t)$, sampling period as $h = 0.01$ s, rapid factor as $r = 120$, the original value as $\{x_1(0) = 0.2, x_2(0) = -1\}$, and $\gamma(t)$ as the evenly distributed white noise with intensity as 0.001. Based on the discrete model of (4), the analysis and comparison of the three algorithms *Fhan*, *Fhan*1, and *Ftd* against the earlier mentioned tracking error of sinusoidal signal and differential error of the obtained signal is as in Figures 5 and 6.

As shown in Figure 5, the deviation of algorithm *Fhan*1 is larger and flutter of it is severer while algorithm *Ftd* is closer to *Fhan*. And as Figure 6 shows, the approximate linear algorithm *Ftd* is very close to algorithm *Fhan* and *Fhan*1 has larger deviation and flutter phenomenon. Under the circumstances of input signal having noise, the deviations of both the tracking signal and differential signal for *Fhan*1 are large. To some extent, the differential signal of algorithm *Fhan*1 is unavailable in practical system. In terms of

the plane phase trajectory, the tracking error, and the differential quality, the approximate linear algorithm presented in this paper is closer to algorithm *Fhan* proposed by Han, which is an appropriate improvement to the approximate linear algorithm in [29] of Han.

4. The Application of Optimized TD in the Fault Detection of Acceleration Sensor

4.1. Simulation Analysis of Fault Detection. A model of the electromagnet of low-speed maglev train has been given in the documents [30]. Adopting the current loop feedback and using the practical parameters, the state equation can be shown:

$$\dot{x}(t) = \begin{bmatrix} 0 & 0 & 1 & 0 \\ 0 & 0 & 0 & 1 \\ 2143.7 & 306.25 & 0 & 0 \\ 306.25 & 2143.7 & 0 & 0 \end{bmatrix} x(t) + \begin{bmatrix} 0 & 0 \\ 0 & 0 \\ -3.5178 & -0.5025 \\ -0.5025 & -3.5178 \end{bmatrix} u(t). \quad (12)$$

According to the optimal control theory, the feedback control algorithm can be obtained as follows:

$$u(t) = Kx(t) = \begin{bmatrix} 1218.8 & 0 & 26.5 & -1.9 \\ 0 & 1218.8 & -1.9 & 26.5 \end{bmatrix} x(t), \quad (13)$$

where the state vector is $x(t) = [x_1 \ x_2 \ x_3 \ x_4]$ and the first two elements in the state vector, respectively, indicate the variation of the gap on the left-side and right-side sensor against the steady-state value, namely, the gap deviation. And the last two elements in the state vector, respectively, indicate the vertical speed of train of the left-side and right-side sensor. All tracks of the maglev train during simulation are deemed smooth.

The two single electromagnets in the electromagnet module are symmetrical. Without loss of generality, here take the acceleration sensor of the left-side single electromagnet having fault as an example to simulate. In order to verify the tracking and differential extraction ability in these three algorithms, the parameters in algorithms of *Fhan*, *Fhan*1, and *Ftd* are set with one accord.

Figure 7 to Figure 9 demonstrate the simulation of the left-side signal when system is fault-free. Figure 7 shows the gap deviation and the tracking status of three kinds of tracking differentiators. Figure 8 displays comparison of the gap differential signal gained from three tracking differentiators and the acceleration integral signal. And Figure 9 displays the absolute D-value (residual for short) between the gap differential signal obtained by the three tracking differentiators and the acceleration integral signal.

As shown in Figures 7, 8, and 9, the system is under stable suspension when fault is free. Since the characteristic

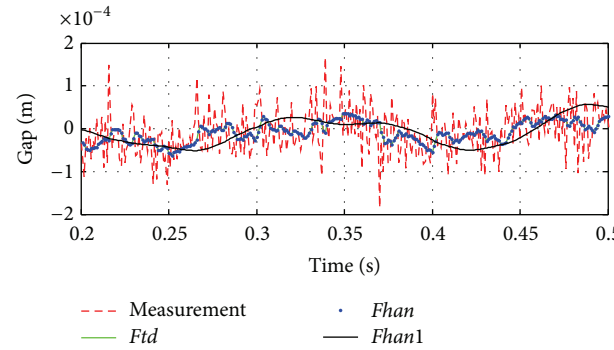

Figure 7: Comparison between the left-side gap deviation and the tracking filtering value without fault.

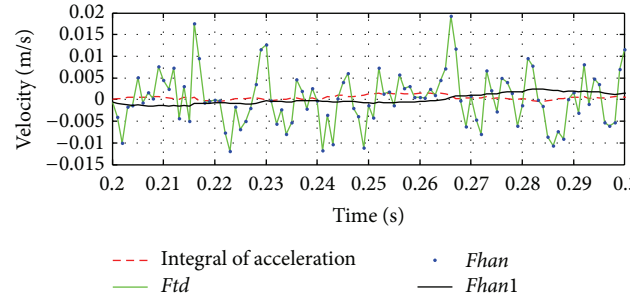

Figure 8: Comparison between the gap differential value and the left-side acceleration integral value without fault.

of maglev train, the gap deviation signal is included the white noise signal that is distributed evenly. In other words, the differential signals and gap signal must have signal-like noise, which is not affected by external disturbance. The simulation results also indicate that *Fhan*1 is very sensitive to noise, and it is unable to process the noise and further obtain the tracking and differential signal. To some degree, *Fhan*1 is not applicable in the maglev train system. A conclusion can be drawn that the tracking and differential extraction ability of the two tracking differentiators in algorithms *Fhan* and *Ftd* are approximate. And both of them have a good filtering effect on the gap signal. In addition, their noise arising from gap differential is also within the minor magnitude.

Figures 10, 11, and 12 demonstrate the simulation results of left-side acceleration sensor when a fault has occurred at 0.5 seconds (i.e., output as 0).

As can be seen from Figure 10, the system begins to shake and diverge when the left-side accelerations sensor fails. But at the same time the tracking differentiator still can track and extract differential signal of the gap signal to a certain extent. However, the tracking and differential extraction of noise signal from algorithm *Fhan*1 is not good according to the simulation results. All the signals obtained from *Fhan*1 algorithm in this system are useless. When the left-side acceleration sensor fails, the acceleration integral value remains the same and it makes gap differential value and the gap signal shake and diverge, which leads to bigger

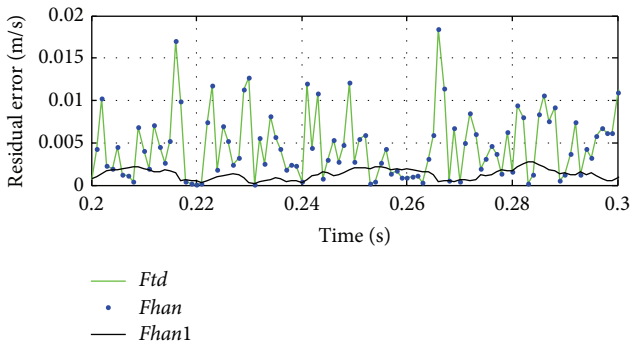

Figure 9: Comparison of the three left-side residuals without fault.

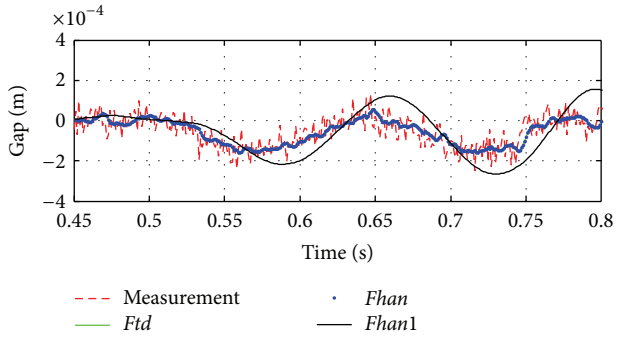

Figure 10: Comparison between the tracking filtering value and gap deviation with acceleration sensor failure.

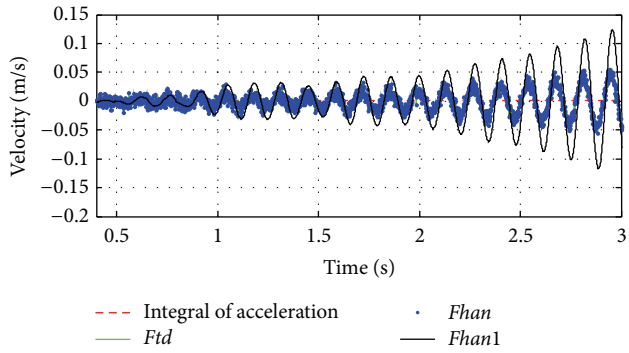

Figure 11: Comparison between gap differential and left-side acceleration integral value with acceleration sensor failure.

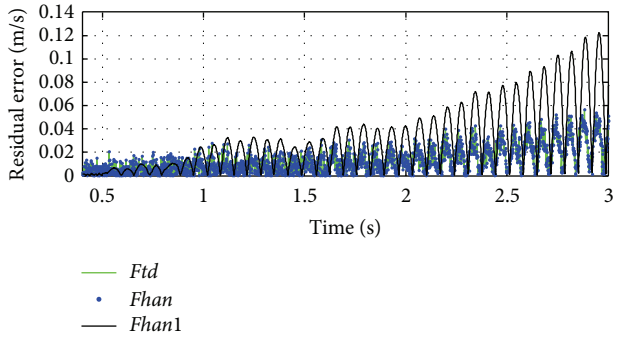

Figure 12: Comparison of three residuals on the left side with acceleration sensor failure.

residual. As can be seen from the result, if the threshold value is set at 0.02, the fault can be detected at 0.52 seconds.

4.2. Threshold Selection. The selection of the earlier mentioned threshold is largely subjective. In order to improve the instantaneity of fault detection and to decline the false alarm rate, it is necessary to introduce an approach of threshold selection that is practical and objective. This paper calculates threshold based on the Bayesian Decision Theory [17]. The algorithm is as follows:

(1) calculation of the mean value and variance of the residual in normal state:

$$\mu_{e0} = \frac{1}{N_{w1}} \sum_{i=1}^{N_{w1}} r(i), \qquad \sigma_0^2 = \frac{1}{N_{w1}} \sum_{i=1}^{N_{w1}} [r(i) - \mu_{e0}]^2, \quad (14)$$

where $r(i)$ indicates the residual sequence in normal state and N_{w1} indicates the data window length;

(2) calculation of all types of statistical property of residual when the system is running:

$$\mu_e = \frac{1}{N_{w1}} \sum_{i=1}^{N_{w1}} r(k-i),$$

$$\sigma_0^2(k) = \frac{1}{N_{w1}} \sum_{i=1}^{N_{w1}} [r(k-i) - \mu_{e0}]^2 \quad (15)$$

$$\sigma_\Pi^2(k) = \frac{1}{N_{w1}} \sum_{i=1}^{N_{w1}} [r(k-i) - \mu_{e0}]^2,$$

where $r(k-1)$ indicates the residual sequence that is waiting for detecting and $N_w \succ N_{w1}$ indicates the data window length;

(3) decision content d and threshold value thr:

$$d_j(k) = \frac{\sigma_I^2(k)}{\sigma_0^2} - \ln \frac{\sigma_\Pi^2(k)}{\sigma_0^2} - 1,$$

$$d_j(k) \begin{cases} \le 2 \ln \left(\dfrac{N_w P_t}{(1-P_t)} \right), & \text{fault-free} \\ \ge 2 \ln \left(\dfrac{N_w P_t}{(1-P_t)} \right), & \text{fault,} \end{cases} \quad (16)$$

where P_t is the prior probability when system is fault-free. According to the experience of practical project, it can be chosen as $P_t = 0.8$. Figure 13 displays the result of threshold by the method mentioned above when it is applied to the residual data.

As can be seen from the simulation result of fault detection in part 4.1, algorithm *Fhan*1 is sensitive to the high-frequency noise signal. And it cannot process noise signal to track or extract the differential signal of the system. As a result, only *Ftd* algorithm has been adopted to do the simulation analysis when decision content and threshold value are analyzed. As shown in the simulation diagram, taking $P_t = 0.8$, the fault on the left-side acceleration sensor can be detected at 0.52 seconds.

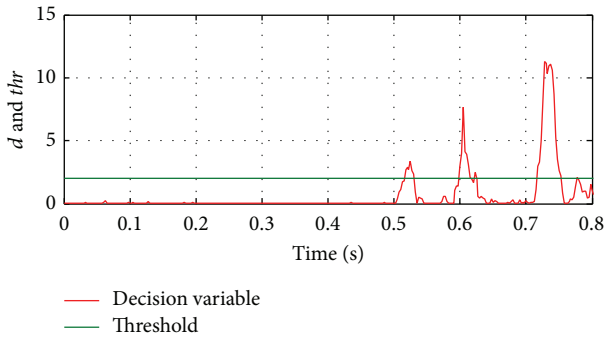

FIGURE 13: Decision content and threshold value.

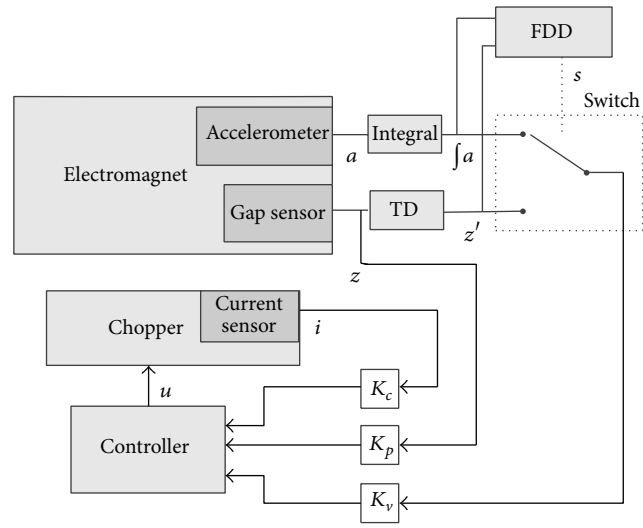

FIGURE 14: Schematic diagram of the fault detection and fault-tolerant control scheme for acceleration sensor.

5. Fault-Tolerant Control of Acceleration Sensor

As can be seen from part 2, it is much likely to break down in acceleration sensor in the suspension control system of maglev train. Fault-tolerant control can be conducted by replacing the acceleration integral signal with the gap differential signal extracted by the optimized approximate linear tracking differentiator when the acceleration sensor fails. The specific schematic diagram of the scheme is shown in Figures 1–5, where gap differential z' is the gap signal processed by differentiator and acceleration integrated signal, $\int a$ is acceleration signal processed by integrator, and decision content d and threshold value thr are processed by the fault detection unit based on the difference between z' and $\int a$. Signal s is obtained based on the relationship between d and thr. The controller then makes the choice between z' and $\int a$ according to the difference of s. $\int a$ is regarded as the velocity feedback when system is normal but when fault is detected in accelerometer by fault detection unit, z' is regarded as the velocity feedback. Thus fault-tolerant control of accelerometer fault is realized. Figure 14 shows the introduction of the speed signal z' obtained from the tracking differentiator into the closed loop feedback control after the acceleration sensor fails during the experiment. The result shows that the introduction of the speed signal obtained from the tracking differentiator into the feedback control can stabilize the system, which is fault-tolerant control.

Figure 15 shows the ultimate gap deviation curve after introducing the speed signal z' obtained by Ftd algorithm when the acceleration sensor fails during experiment. Figure 16 shows the ultimate absolute stable gap value (the suspension gap is between 4.53 mm and 4.54 mm when the maglev train is in stable state) after introducing the fault-tolerant control. During the experiment, the closure of acceleration sensor power is performed to simulate the fault of acceleration sensor. And then speed signal z' is introduced at the first second when the system detects fault. The experimental result shows that the introduction of the speed signal acquired from the tracking differentiator into the feedback control can make system stable.

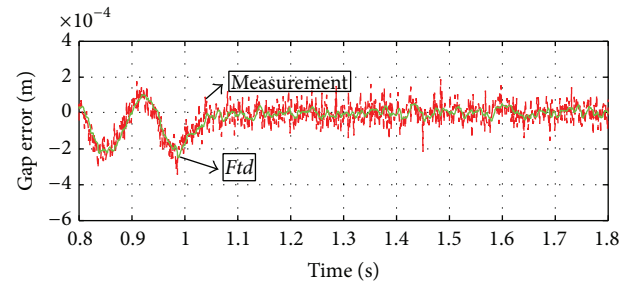

FIGURE 15: The experimental curve of the actual gap error after introducing the fault-tolerant control when acceleration sensor fails.

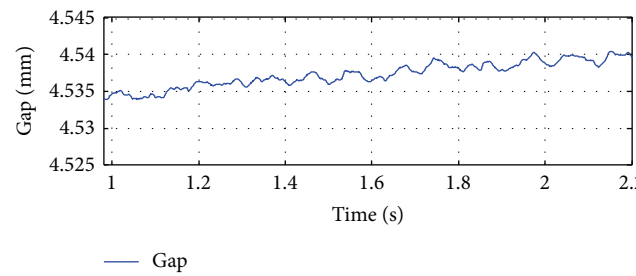

FIGURE 16: The experimental curve of the actual absolute gap after introducing the fault-tolerant control when acceleration sensor fails.

6. Conclusion

This paper focuses on the fault detection of the acceleration sensor for the suspension system of maglev train. The paper studies the approximate linear tracking differentiator proposed by Han during acquiring the speed reference signal and presents a new approximate linear tracking differentiator based on the correction of the disadvantages of this differentiator. Numerical simulation of given signal shows that Ftd algorithm with simple form (without the square roots algorithm) can quickly track an input signal without

chattering and can produce a good differential signal, which is easy to realize in practical application. According to the experiment, fault-tolerant control by using the speed signal obtained from *Ftd* algorithm when the acceleration sensor fails is feasible.

Conflict of Interests

The authors declare that there is no conflict of interests regarding the publication of this paper.

References

[1] Z.-R. Liu, "Commercialization of HSST, an access line of for the 2005 world exposition in Aichi Japan," *Converter Technology & Electric Traction*, vol. 3, no. 1, pp. 50–52, 2005.

[2] R.-J. Wai, J.-D. Lee, and K.-L. Chuang, "Real-time PID control strategy for maglev transportation system via particle swarm optimization," *IEEE Transactions on Industrial Electronics*, vol. 58, no. 2, pp. 629–646, 2011.

[3] E. Kong, J.-S. Song, B.-B. Kang, and S. Na, "Dynamic response and robust control of coupled maglev vehicle and guideway system," *Journal of Sound and Vibration*, vol. 330, no. 25, pp. 6237–6253, 2011.

[4] S. Banerjee, M. K. Sarkar, P. K. Biswas, R. Bhaduri, and P. Sarkar, "A review note on different components of simple electromagnetic levitation systems," *IETE Technical Review*, vol. 28, no. 3, pp. 256–264, 2011.

[5] Y. Li, G. He, and J. Li, "Nonlinear robust observer-based fault detection for networked suspension control system of maglev train," *Mathematical Problems in Engineering*, vol. 2013, Article ID 713560, 7 pages, 2013.

[6] Y. Li, J. Li, G. Zhang, and W.-J. Tian, "Disturbance decoupled fault diagnosis for sensor fault of maglev suspension system," *Journal of Central South University*, vol. 20, no. 6, pp. 1545–1551, 2013.

[7] Z. Q. Long, Z. Q. Lv, S. Huan, and W. S. Chang, "Analysis and design in safeties and reliabilities of the suspension system of Maglev train," in *Proceedings of the 5th World Congress on Intelligent Control and Automation (WCICA '04)*, pp. 1819–1823, HangZhou, China, June 2004.

[8] Z.-Q. Long, Y. Cai, and J. Ye, "Analysis of the reliabilities of maglev train power system with DFTA method," in *Proceedings of the 19th International Conference on Magnetically Levitated Systems and Linear Drives (MAGLEV '2006)*, pp. 449–502, Dresden, Germany, September 2006.

[9] K. Michail, A. Zolotas, R. Goodall, and J. Pearson, "Fault tolerant control for EMS systems with sensor failure," in *Proceedings of the 17th Mediterranean Conference on Control Automation*, pp. 712–717, Thessaloniki, Greece, June 2009.

[10] H. K. Sung, S. H. Lee, and Z. Bien, "Design and implementation of a fault tolerant controller for EMS systems," *Mechatronics*, vol. 15, no. 10, pp. 1253–1272, 2005.

[11] H. K. Sung, D. S. Kim, H. J. Cho, M. H. Yoo, B. S. Kim, and J. M. Lee, "Fault tolerant control of electromagnetic levitation system," in *Proceedings of the 18th Magnetically Levitated System and Linear Drives Conference (MAGLEV '04)*, pp. 676–688, 2004.

[12] H.-J. Kim, C.-K. Kim, and S. Kwon, "Design of a fault-tolerant levitation controller for magnetic levitation vehicle," in *Proceedings of the International Conference on Electrical Machines and Systems (ICEMS '07)*, pp. 1977–1980, October 2007.

[13] Z. Q. Long, S. Xue, Z.-Z. Zhang, and Y.-D. Xie, "A new strategy of active fault-tolerant control for suspension system of maglev train," in *Proceedings of the IEEE International Conference on Automation and Logistics (ICAL '07)*, pp. 88–94, August 2007.

[14] J. Chen and R.-J. Patton, *Robust Model-Based Fault Detection for Dynamic Systems*, Kluwer Academic Publishers, Boston, Mass, USA, 1999.

[15] P.-M. Frank, "Fault diagnosis in dynamic systems using analytical and knowledge-based redundancy—a survey and some new results," *Automatica*, vol. 26, no. 3, pp. 459–474, 1990.

[16] J. Q. Han and L. L. Yuan, "The discrete form of a tracking-differentiator," *Journal of Systems Science and Mathematical Sciences*, vol. 19, no. 3, pp. 268–273, 1999.

[17] T. Bayes, "An essay toward solving a problem in the doctrine of chances," *Philosophical Transactions of the Royal Society of London*, vol. 53, pp. 370–418, 1763.

[18] J. W. Sheppard and M. A. Kaufman, "A Bayesian approach to diagnosis and prognosis using built-in test," *IEEE Transactions on Instrumentation and Measurement*, vol. 54, no. 3, pp. 1003–1018, 2005.

[19] H.-K. Khalil, "Robust servomechanism output feedback controllers for feedback linearizable systems," *Automatica*, vol. 30, no. 10, pp. 1587–1599, 1994.

[20] A. N. Atassi and H. K. Khalil, "Separation results for the stabilization of nonlinear systems using different high-gain observer designs," *Systems & Control Letters*, vol. 39, no. 3, pp. 183–191, 2000.

[21] A. Levant, "Robust exact differentiation via sliding mode technique," *Automatica*, vol. 34, no. 3, pp. 379–384, 1998.

[22] A. Levant, "Higher-order sliding modes, differentiation and output-feedback control," *International Journal of Control*, vol. 76, no. 9-10, pp. 924–941, 2003.

[23] A. Levant, "Sliding order and sliding accuracy in sliding mode control," *International Journal of Control*, vol. 58, no. 6, pp. 1247–1263, 1993.

[24] A. Levant, "Principles of 2-sliding mode design," *Automatica*, vol. 43, no. 4, pp. 576–586, 2007.

[25] V.-I. Utkin, J. Guldner, and J. Shi, *Sliding Mode in Control in Electromechanical Systems*, Taylor & Francis, London, UK, 1999.

[26] V. I. Utkin and A. S. Poznyak, "Adaptive sliding mode control with application to super-twist algorithm: equivalent control method," *Automatica*, vol. 49, no. 1, pp. 39–47, 2013.

[27] J.-Q. Han, "From PID technique to active disturbances rejection control technique," *Control Engineering of China*, vol. 19, no. 3, pp. 13–18, 2002.

[28] Y. D. Xie, Y. G. Li, Z. Q. Long, and C. C. Dai, "Discrete second-order nonlinear tracking-differentiator based on boundary characteristic curves and variable characteristic points and its application to velocity and position detection system," *Acta Automatica Sinica*, vol. 40, no. 5, pp. 952–964, 2014.

[29] J.-Q. Han, *Active Disturbance Rejection Control: The Technique for Estimating and Compensating the Uncertainties*, National Denfence Industry Press, 2008.

[30] D.-S. Liu, *Research on the Module Suspension Control Problem of the EMS Low-Speed Maglev*, National University of Defense Technology, Changsha, China, 2006.